THE JOURNAL OF PHYSICAL CHEMISTRY B

ARTICLE

pubs.acs.org/JPCB

Accurate Critical Micelle Concentrations from a Microscopic Surfactant Model

Asfaw Gezae Daful,[†] Vladimir A. Baulin,[†,‡] Josep Bonet Avalos,[†] and Allan D. Mackie*[,†]

[†]Departament d'Enginyeria Química, ETSEQ, Universitat Rovira i Virgili, Av. dels Paisos Catalans 26, 43007 Tarragona, Spain

[‡]ICREA, 23 Passeig Lluis Companys, 08010 Barcelona, Spain

ABSTRACT: A single chain mean field theory is used to quantitatively describe the micellization process of the nonionic polyethylene oxide alkyl ether, C_nE_m class of surfactants at 25 °C. An explicit but simple microscopic model with only three interaction parameters is shown to be able to reproduce with high accuracy the critical micelle concentrations of a wide range of head and tail surfactant lengths. In addition, the aggregation number of the micelles is studied, the effect of the number of the hydrophobic and hydrophilic segments on CMC and aggregation number of the micelles are discussed and volume fraction profiles are given.

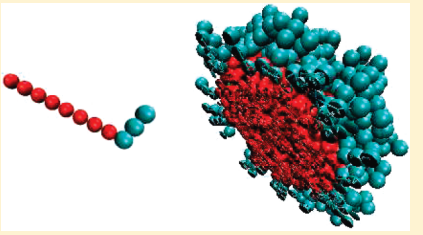

INTRODUCTION

Surfactants are short amphiphilic molecules containing hydrophilic and hydrophobic groups. At low concentrations surfactants form a dilute homogeneous solution of individual molecules, whereas at high concentrations the amphiphilic molecules self-assemble into aggregates or microstructures known as micelles,[1−4] with their hydrophilic groups exposed to solvent and their hydrophobic groups shielded in the micellar interior. The micellization process is governed by the balance of interactions of hydrophobic and hydrophilic groups with the solvent together with the entropic effects due to association. The onset of the aggregation into micelles generally occurs over a narrow range of surfactant concentration and can be quantified by a single concentration value, the critical micelle concentration (CMC).[1] The CMC designates the onset of aggregation of free surfactants into micelles in the spontaneous micellization process emerging over this narrow concentration range. Although the micellization is not a thermodynamic transition, solutions containing surfactants exhibit at the CMC drastic changes in physical and chemical properties such as surface tension, turbidity, conductivity, self-diffusion, osmotic pressure, solubilization, and detergent activity.[3] Thus, the knowledge of precise values of the CMC and an accurate description of the micellization process at the molecular level may be crucial both from a fundamental point of view as well as for practical applications.

The CMC can be determined experimentally by a number of methods, including capillary electrophoresis,[5,6] tensiometry,[7,8] conductometry,[9] fluorescence anisotropy probe,[10] light scattering,[11,12] fluorimetry,[13,14] calorimetry,[15] spectrophotometry,[16] ion-selective electrodes,[17] and nuclear magnetic resonance (NMR) spectroscopy.[18]

The micellization of surfactants has been intensively studied theoretically with a number of analytical models and computer simulations. Nagarajan et al.[19−21] and Blankschtein et al.[22,23] introduced a molecular thermodynamic modeling approach that allows for the prediction of several thermodynamic properties of self-assembled systems, including the CMC and phase behavior. In this approach, the free energy of formation of the micelle, that is, the free-energy change associated with transferring a free surfactant in aqueous solution to a micellar aggregate, is obtained as the sum of several phenomenological free energy contributions[21] such as the transfer free energy, interfacial free energy, packing free energy contribution, the steric free energy and the electrostatic free energy. An a priori estimate needs to be made about how the surfactant molecules will position and orient themselves within the preassembled micellar aggregate and a knowledge of the chemical structure of the surfactant is required to get the free energy contributions. Blankschtein et al.[24] applied molecular dynamics (MD) simulations at an oil/water interface to identify what portions of the surfactant should be modeled as the head and what portions should be modeled as the tail in the context of the molecular-thermodynamic theories of micelle formation.

Monte Carlo (MC) simulations of amphiphilic solutions in lattices have also been used extensively to study the micellization behavior of different types of amphiphiles in solution.[25−31] Panagiotopoulos et al.[31] determined the phase behavior and micellization of several lattice diblock and triblock surfactants using the Larson model[25,26] by histogram-reweighting grand canonical MC simulations. Mackie et al.[27] studied the micelle size, CMC and other thermodynamic properties of a model linear surfactants, H_4T_4 using Monte Carlo simulation and a Single Chain Mean Field (SCMF) theory.[32] Apart from MC simulations, MD simulations[33−38] have proven to be very effective for simulating all-atom and coarse grained models, offering a direct link between chemical structures of surfactants and the micellization process. However, obtaining the free energy of formation of the micelle and many other important

Received: October 26, 2010
Revised: February 7, 2011
Published: March 16, 2011

equilibrium properties like the CMC from MC and MD simulations is computationally expensive.

Scheutjens and Fleer proposed a mean field approach[39,40] to study polymer adsorption in a self-consistent mean field approximation and later Leermakers et al.[41−44] applied this self-consistent field (SCF) theory in order to study the self-assembly of surfactant molecules into micelles. The SCF approach considers the surfactant to be a Gaussian chain in an inhomogeneous mean field ignoring the important intrachain excluded volume interactions. The lattice SCF is computationally efficient and has been used to find the temperature dependence of the lattice model parameters for a collection of pluronic surfactants.[43,45]

One of the theoretical methods that can quantitatively describe the thermodynamics of the micellization process and provide detailed microscopic information about the structure of the micelles is the single chain mean field (SCMF) theory. This method is able to calculate the equilibrium properties for models of surfactant systems at a coarse grained level similar to MC or MD simulations and reproduce the structure of the micelles, the configurations of surfactants and their distribution in the system, the free energy of formation of the micelle and hence, the CMC, the aggregation number and the size distributions of the micelles. Molecular models such as the one used in this work have strong advantages over thermodynamic approaches and we can expect higher transferability not just to other molecules but also to other properties, as well as direct access to all the microscopic information. The SCMF theory was originally developed to study the molecular organization of short amphiphilic molecules in micelles and bilayers assuming dry core aggregates[46−48] or allowing also solvent molecules in the core.[27] The predictions of lattice based SCMF theory[27,32] are in good agreement with MC simulations.

Recently, the SCMF methodology was generalized to study the self-assembly of a mixture of an arbitrary number of types of molecules of an arbitrary structure interacting with each other through mean fields.[49] The SCMF theory and its numerical implementation allows for direct quantitative comparison of equilibrium properties of self-assembled structures with experimental data.[49]

In this paper, we show how an appropriate choice of the microscopic parameters of an explicit microscopic model for surfactant molecules can be used to quantitatively describe the micellization process of the polyoxyethylene alkyl ether, C_nE_m, series of nonionic surfactants at 25 °C. We evaluate the predictive power, precision, and capabilities of our method, by comparing to the large amount of experimental data available for this surfactant and show that the SCMF theory is able to produce with high accuracy the values of the CMC and allows for a description of the micellization thermodynamics at a microscopic level.

We start with the basic equations of the SCMF theory and the micellization process. Furthermore, we present the model that we have used for the C_nE_m surfactant and the manner in which the parameters of this model have been selected. We continue with the discussion of the main results and the predictions of this model for the family of C_nE_m surfactants with different head and tail lengths and compare against experimental results from the literature. Both the ability of the SCMF theory to reproduce the experimental CMC values as well as microscopic details such as the average micellar size and the predicted density profiles of the micelles are discussed. The paper finishes with the conclusions of the most relevant results.

SINGLE CHAIN MEAN FIELD THEORY

The SCMF theory exactly accounts for the configurations of a single microscopically detailed molecule at the molecular level. A molecule of an arbitrary topology[49] can be represented by a coarse grained model along with a corresponding force field at the same level of detail as for MC or MD coarse grained models. In contrast to simulations, the interactions of the molecule with other molecules are described through mean molecular fields. These mean fields (e.g., in the case of surfactants, the concentrations of the hydrophilic and hydrophobic parts of the amphiphilic molecule, and the solvent) are calculated iteratively from the self-consistency condition: individual chain conformations depend on the values of surrounding mean fields, while the values of the fields are obtained as the average properties of the individual conformations. This iterative method converges to the solution which gives the equilibrium structures and the concentration profiles of the molecules and the chain groups as well as the most probable conformations of the molecules. The mean field approximation is valid if there are no strong correlations between interacting particles, such as ion pair formation or bond formation.

In the case of nanosized aggregates freely moving in a solution (e.g., micelles), the translational entropy of the aggregate as a whole can be decoupled from the entropy of molecules moving inside a single aggregate. The SCMF theory can provide an accurate estimate of the full free energy of a single aggregate fixed in the center of the simulation box, while the translational entropy of the aggregates in the system can be accounted through a conventional theory of micellization.

The first step of the SCMF calculations is the definition of a coarse-grained model of a molecule and the interaction of the coarse grained beads with the fields. The proper chain statistics is attained through the direct generation of the representative sampling of conformations Γ of a single molecule. These conformations take into account the angles between the bonds, the orientations and positions of conformations in the simulation box. The free energy, F, of the system containing N surfactant molecules in the mean field approximation is given by

$$\frac{F}{Vk_BT} = \int c(\Gamma) \ln \frac{c(\Gamma)}{e}\Lambda^{3N}\, d\Gamma + \int \frac{d\mathbf{r}}{V} c_s(\mathbf{r}) \ln \frac{c_s(\mathbf{r})}{e}\Lambda_s{}^3 + \int c(\Gamma)u(\Gamma)\, d\Gamma \quad (1)$$

where $c_s(\mathbf{r})$ is the concentration of solvent molecules, the spatial integration is over the volume of the box V, while Λ and Λ_s are the de Broglie lengths of the molecule beads and solvent, correspondingly. Since the correlations between the chains are decoupled, the distribution function of conformations $c(\Gamma)$ is related to the probability of a single molecule conformation $P(\Gamma)$ via $c(\Gamma) = NP(\Gamma)/V$. The function $u(\Gamma)$ represents the interaction potential of the conformation Γ with the fields. The interactions of the beads inside a given conformation, $u_{intra}(\Gamma)$, can be decoupled from the interactions with the fields. Thus, $u(\Gamma)$ can be written as

$$u(\Gamma) = u_{intra}(\Gamma) + \frac{N-1}{2}\int \frac{d\mathbf{r}}{V} P(\Gamma')\hat{u}(\Gamma,\Gamma',\mathbf{r})d\Gamma' + \int \frac{d\mathbf{r}}{V} c_s(\mathbf{r})\tilde{u}(\Gamma,\mathbf{r}) \quad (2)$$

dx.doi.org/10.1021/jp1102302 |J. Phys. Chem. B 2011, 115, 3434–3443

where $\hat{u}(\Gamma,\Gamma',\mathbf{r})$ describes the interactions with the beads of other molecules and $\hat{u}(\Gamma,\mathbf{r})$ describes the interactions with the solvent. The factor 1/2 avoids double counting and $N-1$ is due to the separate intramolecular part.

In the following we consider a surfactant molecule comprising of only two types of beads: hydrophilic, H, and hydrophobic, T. In the case of more complex structures, the equations are easily generalized. Introducing three interaction parameters: between hydrophobic beads and solvent, ε_{TW}, between hydrophilic beads and solvent, ε_{HW}, and between hydrophilic beads and hydrophobic beads, ε_{HT}, the interaction energy yields

$$u(\Gamma) = u_{intra}(\Gamma) + \frac{N-1}{2}\varepsilon_{HT}\int d\mathbf{r}\,[\phi^{H}_{int}(\Gamma,\mathbf{r})\langle c_T(\mathbf{r})\rangle + \phi^{T}_{int}(\Gamma,\mathbf{r})\langle c_H(\mathbf{r})\rangle] + \varepsilon_{TW}\int d\mathbf{r}\,\phi^{T}_{int}(\Gamma,\mathbf{r})\,c_s(\mathbf{r}) + \varepsilon_{HW}\int d\mathbf{r}\,\phi^{H}_{int}(\Gamma,\mathbf{r})\,c_s(\mathbf{r}) \quad (3)$$

where $\phi^{H}_{int}(\Gamma,\mathbf{r})$ and $\phi^{T}_{int}(\Gamma,\mathbf{r})$ are the interaction fields of each conformation in a given position in space. Since the conformations are generated prior to calculations, these properties, as well as the excluded volume of the conformation Γ in a given position of space, $\phi_{ex}(\Gamma,\mathbf{r})$, are known exactly for each conformation. $\langle c_T(\mathbf{r})\rangle$ and $\langle c_H(\mathbf{r})\rangle$ are the average fields of concentrations of T and H, respectively. Average concentrations of each type of the beads and the average volume fraction $\phi(\mathbf{r})$ are calculated as averages of the corresponding concentrations of the conformations as

$$\langle c_T(\mathbf{r})\rangle = \int P(\Gamma)\,c_T(\Gamma,\mathbf{r})\,d\Gamma \quad (4)$$

$$\langle c_H(\mathbf{r})\rangle = \int P(\Gamma)\,c_H(\Gamma,\mathbf{r})\,d\Gamma \quad (5)$$

$$\langle \phi(\mathbf{r})\rangle = \int P(\Gamma)\,\phi_{ex}(\Gamma,\mathbf{r})\,d\Gamma \quad (6)$$

In turn, the volume fraction of solvent is calculated from the incompressibility condition, applied locally as

$$\phi_s(\mathbf{r}) = 1 - N\langle\phi(\mathbf{r})\rangle \quad (7)$$

The probabilities of the conformations $P(\Gamma)$ are found from the minimization of the free energy eq 1 $\delta F\{P(\Gamma)\}/\delta P(\Gamma) = 0$ subject to the incompressibility condition eq 7 imposed by way of the Lagrange multiplier, $\pi(\mathbf{r})$. This gives

$$P(\Gamma) = \frac{1}{Z}e^{-H^{MF}(\Gamma)} \quad (8)$$

where Z is the normalization factor, ensuring $\int P(\Gamma)\,d\Gamma = 1$ and the mean field Hamiltonian H^{MF} given as

$$H^{MF}(\Gamma) = u_{intra}(\Gamma) + (N-1)\varepsilon_{HT}\int d\mathbf{r}\,[\phi^{H}_{int}(\Gamma,\mathbf{r})\langle c_T(\mathbf{r})\rangle + \phi^{T}_{int}(\Gamma,\mathbf{r})\langle c_H(\mathbf{r})\rangle] + \varepsilon_{TW}\int d\mathbf{r}\,\phi^{T}_{int}(\Gamma,\mathbf{r})\frac{\phi_s(\mathbf{r})}{v_s} + \varepsilon_{HW}\int d\mathbf{r}\,\phi^{H}_{int}(\Gamma,\mathbf{r})\frac{\phi_s(\mathbf{r})}{v_s} - \int d\mathbf{r}\,\frac{\phi_{ex}(\Gamma,\mathbf{r})}{v_s}\ln\phi_s(\mathbf{r}) \quad (9)$$

Here we assume that the volume of the beads and the solvent are equal v_s, hence, $\phi_s(\mathbf{r}) = c_s(\mathbf{r})v_s$. The minimization with respect to the concentration of the solvent, $\delta F/\delta c_s(\mathbf{r}) = 0$, gives the Lagrange multiplier in the form $\pi(\mathbf{r}) \approx -1/v_s \ln\phi_s(\mathbf{r})$. Since we assume the beads T and H are of the same size, the interactions T−H and H−T are symmetrical, thus we have omitted $\int d\mathbf{r}\,(c_T(\Gamma,\mathbf{r})\langle\phi^{H}_{int}(\mathbf{r})\rangle + c_H(\Gamma,\mathbf{r})\langle\phi^{T}_{int}(\mathbf{r})\rangle)$ and multiplied the second term by 2.

Equations 4−9 represent a closed set of nonlinear equations, which can be solved iteratively. The mean molecular fields (eqs 4−6) define the probability of each conformation eq 8 in the fields, while the values of mean fields are calculated as averages over the probabilities of conformations, closing the self-consistency loop. The solution of these equations gives the equilibrium distribution of the molecular fields, probabilities of the conformations, the molecular structure of the equilibrium aggregates, the average size of the aggregates, and the equilibrium free energy.

Calculation of the CMC. The micellization process is not a thermodynamic transition and the micelles coexist with free surfactants over a range of concentrations. That is why there are several definitions for the CMC. We use the Israelachvili definition,[1] and the CMC is taken to be the surfactant concentration at which a line of unit slope passing through the origin intersects the asymptote of the free chain concentration beyond the onset of micellization, in a plot of free surfactants mole fraction versus total surfactant mole fraction.

The mass action model is used in order to calculate the free chain and micellar concentrations following a previous work on CMC estimations from the SCMFT.[32] In particular, the mass action model can be given as

$$X_N = N\left\{X_1\exp\left[-\frac{\mu^{o}_N - \mu^{o}_1}{k_BT}\right]\right\}^N \quad (10)$$

where μ^{o}_N and μ^{o}_1 are respectively the standard chemical potentials for amphiphiles in an aggregate of size, N, and for a free chain, X_N is the mole fraction of surfactant molecules in aggregates of size N, X_1 is the mole fraction of free surfactant chains, k_B is the Boltzmann constant, and T is the temperature.

In this work, we calculate the standard chemical potential by way of the SCMFT, which leads us to the following expression for the difference in standard chemical potential between free chains and micelles of size N:[32]

$$\exp\left(-\frac{\mu^{o}_N - \mu^{o}_1}{k_BT}\right) = \frac{V}{N}\frac{\sum_{\Gamma}\exp\left(-\frac{H^{MF}_N[\Gamma]}{k_BT}\right)/W(\Gamma)}{\sum_{\Gamma}\exp\left(-\frac{H_1[\Gamma]}{k_BT}\right)/W(\Gamma)} \quad (11)$$

where $H^{MF}_N[\Gamma]$ is the mean field Hamiltonian of surfactants in a micelle of size N, $H_1[\Gamma]$ is Hamiltonian for free surfactants in the bulk solution. The sum is over a given sample of chain configurations with statistical weight, $W(\Gamma)$, which here is associated with the Rosenbluth and Rosenbluth algorithm used in generating the chain configurations.[50] A detailed explanation can be found in a previous work.[32]

MODEL OF THE C_nE_m SURFACTANT

Most nonionic surfactants are ethylene oxide adducts where the polyoxyethylene (PEO) moiety is the hydrophilic part of the surfactant molecule. The hydrophobic part can be a variety of apolar moieties including alkyl chains, alkyl benzene and their

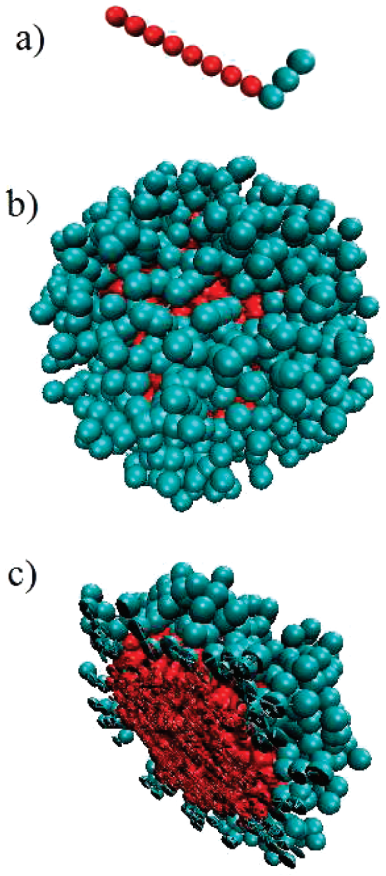

Figure 1. (a) Coarse-grained model of the C_8E_3 surfactant and the resulting mean field "snapshot" (plot of a collection of the most probable conformations) of a spherical micelle comprising of $N = 382$ surfactants, (b) perspective view, and (c) cross-section view. The hydrophobic part is shown as red and the hydrophilic part as light blue.

fluorinated counterparts, silicone derivatives or polyoxypropylene chains. Because many of the experimental CMC values refer to polyoxyethylene alkyl ether surfactants, we chose this surfactant family. Polyoxyethylene alkyl ethers have the general formula, $(C_nH_{2n+1}(OCH_2CH_2)_mOH)$ and are referred to as C_nE_m with n indicating the number of carbons in the alkyl chain and m being the number of ethylene oxide units in the hydrophilic part.

The surfactant molecule is modeled as a linear chain of beads, all of the same size. The distance between the centers of the beads is chosen to correspond to the average distance between the lattice sites in a cubic lattice of coordination 26, i.e., 1.42 of the diameter of the beads. Each tail or T bead represents a CH_2 group of the hydrophobic tail while each head or H bead represents an OCH_2CH_2 group of the hydrophilic head (see Figure 1). We assume that the chain is completely rigid within each Kuhn segment, while the junctions between the segments are free to rotate. The Kuhn segment length[51−54] of polyethylene (alkyl chain) is taken to be 8,[51,54] and that of the oxyethelene chain is set to be 4.[52−54] Such a model of chain rigidity is justified since we are interested in equilibrium properties at the mean field level. The conformations of our model surfactant, are obtained using the Rosenbluth and Rosenbluth chain growth algorithm,[50] which insures self-avoidance of the generated conformations. The resulting bias in the distribution of conformations is corrected with the corresponding weights in the probability of each conformation. From one to four million configurations were used, depending on the simulation box volume, in order to properly sample the single chain configurational space. This sampling was checked by repeating the calculations with double the number of configurations to ensure that the resulting free energy was consistent.

In such a simple model, only three interaction parameters are required: tail−solvent, ε_{TW}, tail−head, ε_{TH}, and head-solvent, ε_{HW}. Furthermore, we estimate the values of the interaction parameters from available experimental data, in order to adjust the parameters as little as possible. Most of the literature data of the interaction parameters of polymers are given in terms of Flory χ parameters[55] defined for a lattice model or related solubility parameters.[56] In our continuous space model, the surfactant beads have an explicit intramolecular hard core repulsion within the bead diameter. The enthalpic contribution is modeled by way of a square well potential which is described by a well interaction energy and additional interaction radius $r_{int.}$[49] Thus, we need to relate our square well potential parameters from continuous space conformations with the lattice model parameters, although this correspondence is not exact due to large difference in the conformational space of the chains between the two models. Interaction volume, v_{int}, of chains in continuous space depends on the conformation, while on a lattice it is a constant. However, we can make a rough approximation by relating the average interaction volume over continuous space conformations with that of a lattice. The interaction volume of a cell in a cubic lattice is equal to its coordination number, $z = 26$. In our continuous space model, the beads of diameter $\sigma = 1$ interact with the neighbors over the interaction range. For an isolated bead the interaction volume $v_{int} = (4/3)\pi(r_{int}^3 - \sigma^3)$, however, if the beads of the chain are close enough, their interaction ranges can overlap, thus making the interaction in the overlapping zones stronger. In order to get a rough correspondence to the lattice model, we have adjusted numerically the value of the interaction radius $r_{int} = 1.61$ of the continuous model to give an average interaction volume per bead $v_{int} = 26$. With this, the interaction parameters are related as $\chi = z\varepsilon/kT$. In addition, the excluded volumes of real space conformations and the chains on the lattice do not match. By matching the free energy for a linear chain composed of $n = 8$ monomers H_4T_4 between lattice and continuous models gives the ratio between the excluded volumes $(\Sigma_\Gamma \int v_{ex}(\Gamma,\mathbf{r})\, d\mathbf{r})/(\Gamma_{tot} n v_s) = 0.885$, where Γ_{tot} is the total number of conformations in the sampling. Hence, the excluded volume contribution (last term in eq 9) should be corrected by the corresponding factor.

A first approximation for the tail-solvent interaction parameter χ_{TW}, is taken from equilibrium solubility data of alkanes in water. The activity coefficient[57] of a solvent a_1 is given by

$$\ln a_1 = \ln(1-\phi_2) + (1-1/r)\phi_2 + \chi_{TW}\phi_2^2 \qquad (12)$$

where ϕ_2 is the volume fraction of the polymer and r is the chain segment number (ratio of polymer to solvent molar volume). Assuming that the alkyl ether tails of the polyoxyethylene alkyl ether surfactants are similar to alkane molecules, we calculated the activity coefficient of alkane chains from the water−-*n*-ethane, water−*n*-propane, water−*n*-butane, water−*n*-pentane, water−*n*-hexane, water−*n*-heptane, water−*n*-octane, water−*n*-nonane, and the water−*n*-decane systems, (alkanes of C_2 to

dx.doi.org/10.1021/jp1102302 |J. Phys. Chem. B 2011, 115, 3434–3443

Table 1. Calculated and Experimental Critical Micelle Concentrations and Micelle Aggregation Numbers of Polyoxyethylene Alkyl Ether Surfactants, C_nE_m, at 25 °C

				experiment			simulation		
				CMC			CMC		
	nonionic surfactant	MW [g/mol]	V_M [mol/L]	[mol/L]	mol frac	N	[mol/L]	mol frac	N
C_nE_3									
	C_6E_3	234	0.227	0.09[61,62]	0.00185		0.075	0.0013	380
	C_7E_3	248	0.245	0.02[61]	3.62×10^{-4}		0.017	3.1×10^{-4}	375
	C_8E_3	262	0.27	0.0075[3,61,62]	1.36×10^{-4}		0.0051	9.2×10^{-5}	370
	$C_{12}E_3$	318	0.32	1.00×10^{-4}[3,61]	9.40×10^{-7}		9.5×10^{-5}	1.7×10^{-6}	975
	$C_{14}E_3$	346	0.374	1.00×10^{-5}[61]	1.80×10^{-7}		1.2×10^{-5}	2.1×10^{-7}	870
	$C_{16}E_3$	374	0.41	1.20×10^{-6}[61]	2.16×10^{-8}		1.6×10^{-6}	2.8×10^{-8}	820
C_nF_4									
	C_6E_4	278	0.266	0.09	0.00167[63]		0.085	0.0016	210
	C_8E_4	306	0.31	0.008[61]	1.56×10^{-4}		0.0090	1.6×10^{-4}	333
	$C_{12}E_4$	363	0.376	6.40×10^{-5}[3,61,64]	1.2×10^{-6}		8.8×10^{-5}	1.6×10^{-6}	905
C_nE_5									
	C_6E_5	322	0.305	0.09[61]	0.00173		0.099	0.0018	140
	C_8E_5	350	0.32	0.009[3,61]	1.77×10^{-4}		0.010	1.8×10^{-4}	260
	$C_{10}E_5$	378	0.39	8.40×10^{-4}[61,65]	1.46×10^{-5}		8.8×10^{-4}	1.6×10^{-5}	908
	$C_{12}E_5$	406	0.41	6.20×10^{-5}[3,61,66]	1.2×10^{-6}		8.8×10^{-5}	1.6×10^{-6}	855
	$C_{14}E_5$	434	0.47	1.00×10^{-5}[61]	1.80×10^{-7}		1.2×10^{-5}	1.8×10^{-7}	840
C_nE_6									
	C_6E_6	366	0.345	0.0695[65]	0.00127		0.12	0.0021	123
	C_8E_6	395	0.39	0.0098[3,61,62,65,66]	1.80×10^{-4}		0.012	2.0×10^{-4}	200
	$C_{10}E_6$	423	0.418	9.00×10^{-4}[3,62,65,66]	1.63×10^{-5}		0.0011	2.0×10^{-5}	470
	$C_{12}E_6$	451	0.45	8.70×10^{-5}[3,61,62,64−66]	1.6×10^{-6}	400	1.0×10^{-4}	1.9×10^{-6}	775
	$C_{16}E_6$	507	0.528	1.00×10^{-6}[3,65]	2.35×10^{-8}	2430	1.3×10^{-6}	2.3×10^{-8}	750
C_nE_7									
	$C_{10}E_7$	467	0.457	9.62×10^{-4}	1.74×10^{-5}[63]		0.0013	2.4×10^{-5}	250
	$C_{12}E_7$	495	0.49	8.20×10^{-5}[3,61]	1.5×10^{-6}		1.3×10^{-4}	2.4×10^{-6}	520
	$C_{16}E_7$	551	0.567	1.70×10^{-6}[3]	3.07×10^{-8}	594	1.5×10^{-6}	2.6×10^{-8}	720
C_nF_8									
	C_8E_8	482	0.459	0.01[61]	1.81×10^{-4}		0.015	2.8×10^{-4}	270
	C_9E_8	497	0.517	0.003[66]	5.43×10^{-5}		0.0045	8.2×10^{-5}	215
	$C_{10}E_8$	511	0.51	1.00×10^{-3}[3,61,66]	1.81×10^{-5}		0.0015	2.7×10^{-5}	250
	$C_{11}E_8$	524	0.52	3.00×10^{-4}[61,66]	5.42×10^{-6}		4.9×10^{-4}	8.8×10^{-6}	310
	$C_{12}E_8$	538	0.54	1.00×10^{-4}[3,61,64,65]	1.28×10^{-6}	123	1.7×10^{-4}	3.0×10^{-6}	380
	$C_{13}E_8$	553	0.571	3.00×10^{-5}[61]	4.88×10^{-7}		5.1×10^{-5}	9.2×10^{-7}	670
	$C_{14}E_8$	567	0.569	9.00×10^{-6}[3,61,66]	1.63×10^{-7}		1.6×10^{-5}	2.9×10^{-7}	780
	$C_{15}E_8$	581	0.588	3.50×10^{-6}[61,66]	6.32×10^{-8}		5.2×10^{-6}	9.2×10^{-8}	760
	$C_{16}E_8$	595	0.606	5.00×10^{-7}[61]	2.17×10^{-8}		1.8×10^{-6}	3.2×10^{-8}	660
C_nF_9									
	C_8E_9	527	0.53	0.013[61,62,66]	2.37×10^{-4}		0.016	2.9×10^{-4}	170
	$C_{10}E_9$	555	0.535	0.00138[62,65,66]	2.35×10^{-5}		0.0018	3.1×10^{-5}	240
	$C_{12}E_9$	583	0.58	8.00×10^{-5}[3,61]	1.81×10^{-6}		1.8×10^{-4}	3.3×10^{-6}	283
	$C_{16}E_9$	639	0.645	2.12×10^{-6}[3,66]	3.79×10^{-8}	219	2.2×10^{-6}	3.9×10^{-8}	570
$C_{12}E_m$									
	$C_{12}E_{10}$	626	0.62	9.00×10^{-5}[61]	1.63×10^{-6}		2.0×10^{-4}	3.6×10^{-6}	270
	$C_{12}E_{11}$	670	0.665				2.5×10^{-4}	4.5×10^{-6}	244
	$C_{12}E_{12}$	714	0.71	1.00×10^{-4}[3,61]	1.80×10^{-6}	81	2.8×10^{-4}	5.0×10^{-6}	293
	$C_{12}E_{13}$	758	0.767	2.00×10^{-4}[61]	3.60×10^{-6}		3.0×10^{-4}	5.5×10^{-6}	284
	$C_{12}E_{23}$	1198	1.12	6.00×10^{-5}[61]	1.08×10^{-6}	40	7.6×10^{-4}	1.4×10^{-5}	215
	$C_{12}E_{25}$	1286	1.2	1.00×10^{-4}[61]	1.80×10^{-6}		6.5×10^{-4}	1.2×10^{-5}	170

dx.doi.org/10.1021/jp1102302 |J. Phys. Chem. B 2011, 115, 3434–3443

C_{10}), at infinite dilution in water at 25 °C, from liquid−liquid equilibrium data of alkane−water systems.[58,59] This activity coefficient in turn is used to calculate the χ_{TW} parameters for each alkane extrapolating the values to infinite dilution of the solvent. These calculations indicated that the χ_{TW} should have a value of approximately 2.5. The interaction parameter of the EO group with water, χ_{HW}, in terms of the Flory lattice model, has a strong concentration dependence.[60] This reflects the conformational dependence of interactions with water and the formation of hydrogen bonds. However, the heads of the surfactant C_nE_m are relatively short and the interactions of the heads groups with water are much weaker than the tail-water interactions. We found a weak dependence of the CMC values for this parameter and no concentration gradient in the corona of micelles. Thus, we used a constant value $\chi_{HW} = 0.5$ to model interactions of EO units with water at 25 °C and did not adjust it further.

In order to refine the approximate value of the tail−solvent parameter,χ_{TW}, and to adjust the value of the χ_{TH}, for which we were unable to find any experimental data, we used an optimization technique, so as to reproduce the experimental CMC value of the following surfactants $C_{10}E_3$, $C_{10}E_6$, $C_{10}E_8$, C_8E_3, C_8E_6, C_8E_8, C_6E_3, C_6E_6, C_6E_8, and $C_{16}E_9$. In particular, a series of simulations was conducted for different values of χ_{TW} and χ_{TH}, i.e., keeping one of these parameters fixed and running simulations with a range of values of the other parameter. The optimization gave us $\chi_{TW} = 2.40$ and $\chi_{TH} = 0.34$. During this process we observed that the CMC is highly sensitive to χ_{TW} and less sensitive to χ_{TH}. For instance a 3% change in χ_{TW} can result in a 100% change of the CMC, whereas a 25% change in χ_{TH} can result in only a 13% change of the CMC.

To summarize, the following parameters, $\chi_{HW} = 0.5$, $\chi_{TW} = 2.40$, and $\chi_{TH} = 0.34$, only two of which are adjusted, have been used to model the CMC and the equilibrium properties of the full family of C_nE_m surfactants given in the following section.

RESULTS AND DISCUSSION

The CMC values obtained from the SCMF theory and the equilibrium sizes of the micelles for a wide range of polyoxyethylene alkyl ether surfactants, C_nE_m, are compared with experimental values from the literature at 25 °C in Table 1, which also includes the molar volume, V_M, and molar weight M_W of the surfactants. The relative errors for the CMCs and aggregation numbers have been calculated for several of the surfactants and are found to be between 1% and 4% for the CMCs and about 1% for the aggregation number. This means that the CMCs and aggregation numbers given in Table 1 are accurate to two significant figures. The CMC in mole fraction, X, is related to the CMC in [mol/L] C from the following relationship, $C = 1/(v_p + v_s(1/X) - 1)$, where v_s and v_p are the molar volumes of the solvent and surfactant, respectively. As can be seen, the CMC values of the present work are in good agreement with the experimental values.

Figures 2 and 3 show the dependence of the CMC on the number of ethylene oxide (head) groups, m, and methylene (tail) groups, n. It is found that varying the length of the tail group for a constant length of the headgroup causes the CMC to decrease exponentially, as can be seen by the linear decrease in the CMC in the log−linear plot in Figure 2. A longer hydrophobic tail length indicates that it is thermodynamically more favorable for the molecule to leave the aqueous solution; that is, increasing the chain length of the hydrophobic alkyl segment n enhances

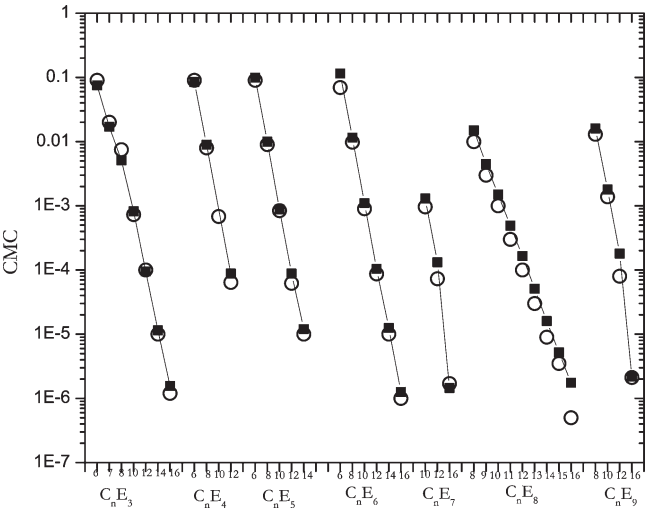

Figure 2. Critical micelle concentration in [mol/L] versus the length of the hydrophobic tail group n for surfactants C_nE_3, C_nE_4, C_nE_5, C_nE_6, C_nE_7, C_nE_8, and C_nE_9. Open circles are experimental data from the literature, while filled squares are values calculated from the SCMF theory values, lines are included to help guide the eye.

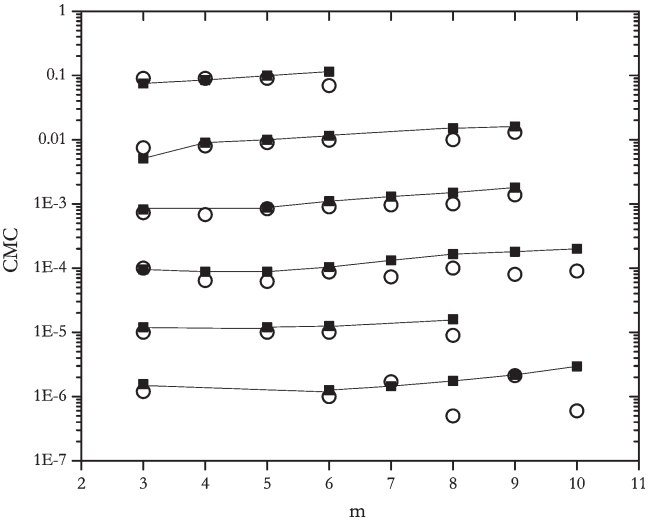

Figure 3. Critical micelle concentration in [mol/L] versus the length of the headgroup, m for C_nE_m surfactants for given tail lengths, n (n = 6, 8, 10, 12, 14, and 16 from top to bottom). Open circles are experimental values from the literature, while filled squares are values calculated from the SCMF theory, lines are included to help guide the eye.

the repulsive hydrocarbon−water interaction. This increases the tendency to push the hydrocarbons out of the aqueous medium. Therefore, this results in the formation of micelles at lower concentrations, and hence reduces the critical micelle concentration.

On the other hand, a longer hydrophilic head length gives the contrary result. The longer the hydrophilic chain the surfactant has, the more soluble it is in aqueous solution, thus reducing the surfactant's tendency to migrate from the bulk to the interface and aggregate into a micelle. For the cases in which the length of the hydrophobic tail remains constant and the length of the hydrophilic head increases, the CMC values increases slightly with increasing the headgroup length. Figure 3 shows

dx.doi.org/10.1021/jp1102302 |J. Phys. Chem. B 2011, 115, 3434–3443

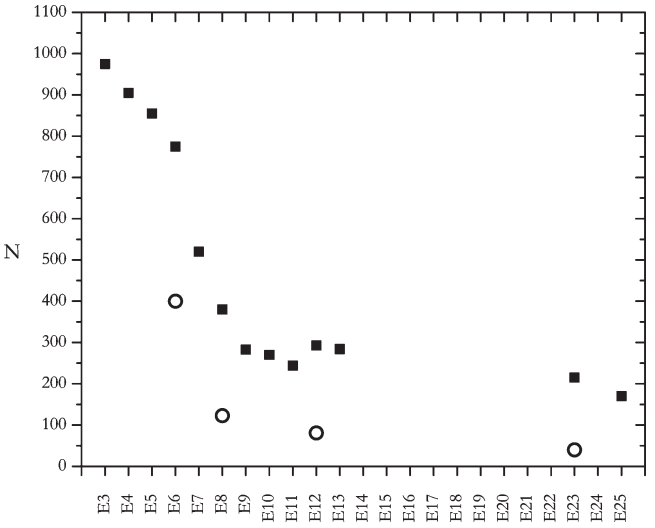

Figure 4. Effect of the number of oxyethylene monomers, *m*, on the aggregation number for the polyoxyethylene alkyl ether surfactants of hydrophobic length 12, $C_{12}E_m$, in a log−linear plot. Open circles represent literature experimental values while filled squares represent SCMFT simulation values from this work.

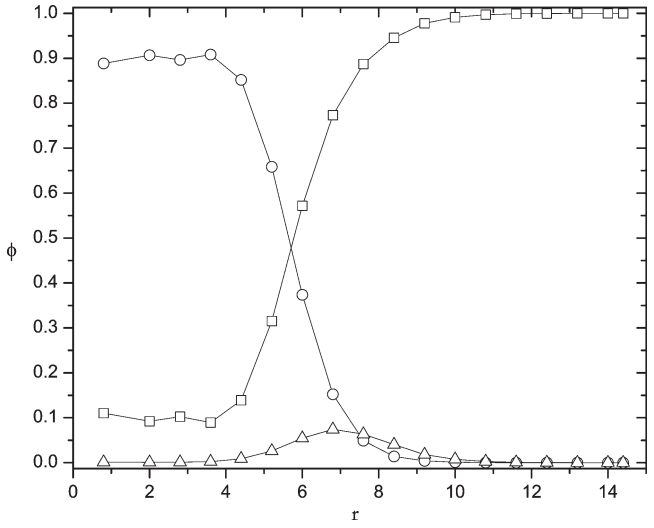

Figure 5. Radial distribution of volume fraction profiles for the $C_{16}E_3$ surfactant for a micelle of size $N = 100$: tail (circles), head (triangles), and solvent (squares).

experimental and SCMFT simulation CMC values of the surfactants C_nE_m, where the length of the tail *n* is kept constant and the length of the head, *m* increases. As can be seen, the CMC increases with the length of the headgroup *m* for all C_nE_m. The SCMFT simulation predicts a smoother trend for the CMC with increasing number of hydrophilic monomers as compared with the literature experimental values, this is particularly the case for the long hydrophobic tails (C_{12}, C_{14}, and C_{16}). In addition we observe that the change of the CMC value per oxyethylene unit in the hydrophilic head is much smaller than that per methylene unit in the hydrophobic tail.

In agreement with geometric considerations from packing parameters,[3] the aggregation numbers in aqueous solution increase with an increase in the length of the hydrophobic group and decrease with respect to an increase in the number of hydrophilic units. Figure 4 shows the variation of the aggregation number with the length of the hydrophilic segment, *m*, of the surfactant, $C_{12}E_m$, for both experimental data from the literature and the SCMFT calculation. As can be observed, the SCMFT significantly overestimates the size of the micelles as compared with the experimental data. However, the qualitative trend agrees in the sense that as the head or hydrophilic segment increases, the aggregation number drops at first quickly and then more slowly.

Although the SCMFT has been found to give results for the free energy and hence the CMC in quantitative agreement with Monte Carlo simulation results for the same model,[27] significant differences have been found for the aggregation number. This may be due to various causes in our mean field approximation such as the lack of fluctuations for a relatively flat free energy landscape or the imposition of a spherical micellar geometry. It can be expected that the micellar size is controlled by relatively small differences in free energy and is hence sensitive to these effects whereas the overall free energy difference for micelle formation, which is responsible for the CMC, is much larger and is not susceptible to such details. In addition, since in this work we compare with experimental data, the choice of the microscopic model and the interaction parameters used is also a factor.

It is of course expected that the hydrophobic part of the surfactant will concentrate in the center of the micelle, to maximize the number of tail−tail contacts, so that the hydrophilic parts be expelled to the outer regions of the micelle. Such a behavior has indeed been observed in previous simulations and is also found in this work. As already mentioned, micelles consist of a core of hydrophobic chains shielded from contact with water by hydrophilic head groups. The hydrophilic units of surfactants form a micellar corona. This can be seen in the configuration plot of a spherical micelle of C_8E_3 with aggregation number $N = 382$ and its cross-sectional view in Figure 1. Please note that this is plotted by selecting the most probable conformations so as to give a general idea of the micelle and, although the individual chain configurations are correct, it does not include excluded volume interactions between surfactants.

In Figures 5 and 6 the radial volume fraction profiles of a micelle of size $N = 100$ and 1000 respectively are given for the $C_{16}E_3$ surfactant. As can be seen from the plots, the core of the micelle is predominantly occupied by the tail segments, with the hydrophilic head segments at the interface between the tail segments and the bulk water where it has a maximum. Figure 5 is typical of micellar distribution plots for spherical micelles found in this and other simulation studies and has an approximately constant value of the different tail and head segments away from the interfacial zone inside the micelle core. However, in the case of the larger micelles found in this work for aggregation sizes greater than ($N \sim 400$), a different behavior is observed. In particular, the volume fraction of tail segments drops toward the center of the micelle and that of the head segments increases. This is no doubt due to fact that as the volume and hence diameter of the micelle core becomes larger, at some point the tails are not able to reach the center while maintaining the head at the surface. Normally this forces the free energy of the micelle to increase and makes the larger micelles unfavorable. However, due to the interaction parameters used in this work, namely that the tail−head interaction is more favorable than the tail-water one, it is found that an even more stable conformation can be found in some cases by placing the heads in the center as well as at the interface. This can be seen from the

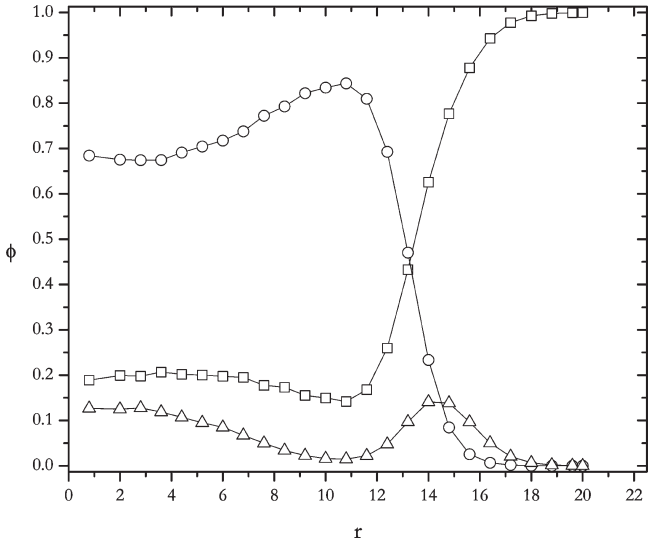

Figure 6. Radial distribution of volume fraction profile for the $C_{16}E_3$ surfactant for a micelle of size $N = 1000$: tail (circles), head (triangles), and solvent (squares).

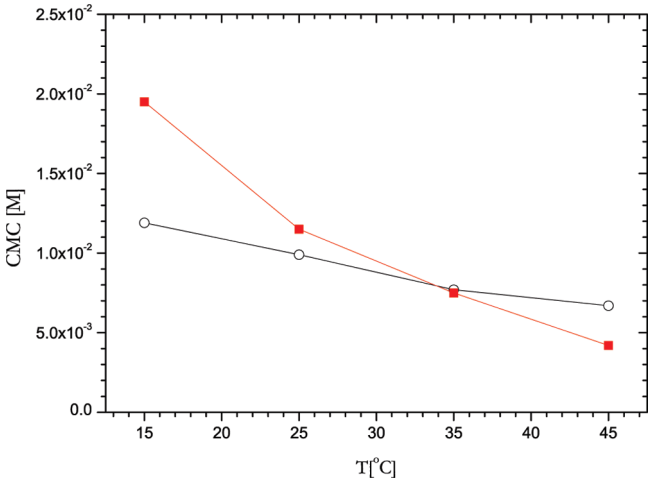

Figure 7. CMC values of C_8E_6 as a function of temperature: experimental values (circles), simulation values (squares).

plots of the volume fraction profiles given in Figure 6 for a micelle of size $N = 1000$ where the head volume fraction reaches a second maximum in the center of the micelle, a "prevesicular" micelle.

With regards to the experimental data available, a wide range of micelle aggregation numbers from less than a hundred to several thousand have been reported for these surfactants (see Table 1); however, it is not clear what geometrical form these micelles have. The SCMFT calculations carried out here assume a spherical geometry which may not be consistent with the experimental system. It is also possible to carry out calculations for other one or two-dimensional geometries in the SCMFT, however these calculations have not been carried out in this work since the main focus here is on reproducing the CMC values. In addition, variations in the interaction parameters may affect the relative stability of these large micelles, where the balance between the tail−head and tail−water interaction is certainly important. The tail−head interaction is not available experimentally and is difficult to fix. These effects can change the size of the preferred aggregation number as small changes of the order of a fraction of a kT are important, and so the simulation data for aggregation number should be treated with caution. However, the CMC is controlled by free energy differences of several kT and is not expected to be significantly affected.

We have also investigated the temperature dependence of the CMC and aggregation number for several of the surfactants. Here we assume that the model χ parameters should have an inverse temperature dependence. In Figure 7 a plot of the CMC for C_8E_6 is given as a function of temperature along with the available experimental data where we have modified our original χ parameters accordingly. As can be seen, we obtain a similar behavior with a decrease in the CMC with temperature as expected. However, the model over predicts the rate of this change. We also find the correct qualitative behavior for the increase in aggregation number with temperature.[67] In fact, it is well-known that such an inverse dependence is adequate only for simple solvents and that the hydrogen bonding characteristics of water make it more difficult to model. Experimental data for the temperature dependence of hydrocarbons in water is available[58] and, together with additional information for the temperature dependence of the headwater and head tail interaction, it should be possible to obtain an improved temperature dependence.

CONCLUSIONS

In this work, the single chain mean field theory has been applied to quantitatively reproduce the critical micelle concentration values of a wide range of nonionic polyoxyethylene alkyl ether surfactants, C_nE_m, with a single set of three parameters. The main objective was to develop an explicit but simple microscopic model within our SCMFT simulation methodology in order to capture the micellization process. In particular, a three interaction parameter continuous space model has been chosen. The headwater interaction was taken from literature experimental work, whereas the tail−water interaction was estimated from alkane−water solubility data. An optimization method was then applied to fine-tune the tail−water interaction and fit the head−tail interaction, for which no experimental information could be found. The resulting SCMFT model has been shown to successfully reproduce the experimental critical micelle concentrations of polyoxyethylene alkyl ether surfactants in water. As expected, the cmc values decrease exponentially with increasing surfactant tail length, whereas it slightly increases with an increase of the head length of the surfactant.

In addition, certain microscopic properties were also calculated and analyzed. These include the micellar volume fraction profiles as well as the preferred aggregation number, where it was found that increasing the alkyl chain (tail) length or decreasing the poly(oxyethylene) chain (head) length causes an increase in the micelle aggregation number in qualitative agreement with experiment. However, the SCMFT was found on the whole to overestimate the aggregation number and is expected to be sensitive to the details of the model used as well as to the mean-field nature of our approach.

Further effort is required to check assumptions such as the imposed spherical geometry of the micelles or the particular values of the head−tail interaction parameters, particularly for the larger micelles of more than approximately four hundred surfactants. To conclude, this work offers interesting perspectives for the use of an explicit microscopic model with the single chain mean field theory

to quantitatively model the micellization process and give accurate values for the critical micelle concentrations.

AUTHOR INFORMATION

Corresponding Author
*E-mail: allan.mackie@urv.cat.

ACKNOWLEDGMENT

The authors acknowledges financial help from Spanish Ministry of education MICINN via Project CTQ2008-06469/PPQ and the U.K. Royal Society for an International Joint Project with Cambridge University, U.K.

REFERENCES

(1) Israelachvili, J. *Intermolecular and Surface Forces*, 7th ed.; Academic Press, San Diego, CA, 1998.
(2) Holmberg, K.; Jonsson, B.; Kronberg, B.; Lindman, B. *Surfactants and Polymers in Aqueous Solution*, 2nd ed.; John Wiley & Sons, Ltd.: New York, 2002.
(3) Rosen, M. J. *Surfactants and Interfacial Phenomena*; John Wiley & Sons, Ltd.: New York, 2004.
(4) Hamley, I. W. *Introduction to Soft Matter*; John Wiley & Sons, Ltd.: New York, 2007.
(5) Lin, C.-E.; Fang, I.-J.; Deng, Y.-J.; Liao, W.-S.; Cheng, H.-T.; Huang, W.-P. *J. Chromatogr. A* **2004**, *1051*, 85–94.
(6) Stanley, F. E.; Warner, A. M.; Schneiderman, E.; Stalcup, A. M. *J. Chromatogr. A* **2009**, *1216*, 8431–8434.
(7) Zheng, Z.; Obbard, J. P. *Water Res.* **2002**, *36*, 2667–2672.
(8) Calvo, E.; Bravo, R.; Amigo, A.; Gracia-Fadrique, J. *Fluid Phase Equilib.* **2009**, *282*, 14–19.
(9) Sifaoui, H.; Lugowska, K.; Domanska, U.; Modaressi, A.; Rogalski, M. *J. Colloid Interface Sci.* **2007**, *314*, 643–650.
(10) Thorsteinsson, M. V.; Richter, J.; Lee, A. L.; DePhillips, P. *Anal. Biochem.* **2005**, *340*, 220–225.
(11) Paillet, S.; Grassl, B.; Desbrieres, J. *Anal. Chim. Acta* **2009**, *636*, 236–241.
(12) Reis, S.; Moutinho, C. G.; Matosa, C.; de Castro, B.; Gameiro, P.; Lima, J. L. *Anal. Biochem.* **2004**, *334*, 117–126.
(13) Zhang, X.; Jackson, J. K.; Burt, H. M. *J. Biochem. Biophys. Methods* **1996**, *31*, 145–150.
(14) Hara, K.; Kuwabara, H.; Kajimoto, O.; Bhattacharyya, K. *J. Photochem. Photobiol., A* **1999**, *124*, 159–162.
(15) Li, Z.; Mintzer, E.; Bittman, R. *Chem. Phys. Lipids* **2004**, *130*, 197–201.
(16) Li, N.; Luo, H.; Liu, S. *Spectrochim. Acta Part A* **2004**, *60*, 1811–1815.
(17) López-Fontan, J. L.; Gonzalez-Perez, A.; Costa, J.; Ruso, J. M.; Prieto, G.; Schulz, P. C.; Sarmiento, F. *J. Colloid Interface Sci.* **2006**, *294*, 458–465.
(18) Kjellin, U. R. M.; Reimer, J.; Hansson, P. *J. Colloid Interface Sci.* **2003**, *262*, 506–515.
(19) Ruckenstein, E.; Nagarajan, R. *J. Phys. Chem.* **1981**, *85*, 3010–3014.
(20) Nagarajan, R. *Langmuir* **1985**, *1*, 331–341.
(21) Nagarajan, R. *Langmuir* **1991**, *7*, 2934–2969.
(22) Zoeller, N.; Lue, L.; Blankschtein, D. *Langmuir* **1997**, *13*, 5258–5275.
(23) Reif, I.; Mulqueen, M.; Blankschtein, D. *Langmuir* **2001**, *17*, 5801–5812.
(24) Stephenson, C. B.; Beers, K.; Blankschtein, D. *Langmuir* **2006**, *22*, 1500–1513.
(25) Larson, R. G.; Scriven, L. E.; Davis, H. T. *J. Chem. Phys.* **1985**, *83*, 2411–2420.
(26) Larson, R. G. *J. Chem. Phys.* **1988**, *89*, 1642–1650.
(27) Mackie, A. D.; Panagiotopoulos, A. Z.; Szleifer, I. *Langmuir* **1997**, *13*, 5022–5031.
(28) Nelson, P. H.; Rutledge, G. C.; Hatton, T. A. *J. Chem. Phys.* **1997**, *107*, 10778–10781.
(29) Floriano, A. M.; Caponetti, E.; Panagiotopoulos, A. Z. *Langmuir* **1999**, *15*, 3143–3151.
(30) Gharibi, H.; Hashemianzadeh, S.; Razavizadeh, B. *Physicochem. Eng. Aspects* **2002**, *196*, 31–38.
(31) Panagiotopoulos, A. Z.; Floriano, M. A.; Kumar, S. K. *Langmuir* **2002**, *18*, 2940–2948.
(32) Al-Anber, Z. A.; Bonet-Avalos, J.; Mackie, A. D. *J. Chem. Phys.* **2005**, *122*, 104910.
(33) Marrink, S. J.; Tieleman, D. P.; Mark, A. E. *J. Phys. Chem. B* **2000**, *104*, 12165–12173.
(34) Yoshii, N.; Iwahashi, K.; Okazakia, S. *J. Chem. Phys.* **2006**, *124*, 184901.
(35) Jian, G.; Ying, R.; Wei, G. *Chin. J. Chem. Eng.* **2009**, *17*, 654–660.
(36) Shang, B. Z.; Wang, Z.; Larson, R. G. *J. Phys. Chem. B* **2008**, *112*, 2888–2900.
(37) Sammalkorpi, M.; Karttunen, M.; Haataja, M. *J. Phys. Chem. B* **2007**, *111*, 11722–11733.
(38) Khurana, E.; Nielsen, S. O.; Klein, M. L. *J. Phys. Chem. B* **2006**, *110*, 22136–22142.
(39) Scheutjens, J. M. H. M.; Fleer, G. *J. Am. Chem. Soc.* **1979**, *83*, 1619–1635.
(40) Scheutjens, J. M. H. M.; Fleer, G. J. *J. Phys. Chem.* **1980**, *84*, 178–190.
(41) Leermakers, F. A. M.; Scheutjens, J. M. H. M. *J. Phys. Chem.* **1989**, *93*, 7417–7426.
(42) Leermakers, F. A. M.; Wijmans, C. M.; Fleer, G. J. *Macromolecules* **1995**, *28*, 3434–3443.
(43) de Bruijn, V.; van den Broeke, L. J. P.; Leermakers, F. A. M.; Keurentjes, J. T. F. *Langmuir* **2002**, *18*, 10467–10474.
(44) Lauw, Y.; Leermakers, F. A. M.; Stuart, M. A. C. *J. Phys. Chem.* **2003**, *107*, 10912–10918.
(45) Hurter, P. N.; Scheutjens, J. M. H. M.; Hatton, T. A. *Macromolecules* **1993**, *26*, 5592–5601.
(46) Ben-Shaul, A.; Gelbart, W. M.; Szleifer, I. *Proc. Natl. Acad. Sci. U. S.A.* **1984**, *81*, 4601–4605.
(47) Ben-Shaul, A.; Gelbart, W. M.; Szleifer, I. *J. Chem. Phys.* **1985**, *83*, 3597–3611.
(48) Szleifer, I.; Ben-Shaul, A.; Gelbart, W. M. *J. Chem. Phys.* **1985**, *83*, 3612–3620.
(49) Pogodin, S.; Baulin, V. A. *Soft Matter* **2010**, *6*, 2216–2226.
(50) Rosenbluth, M. N.; Rosenbluth, A. W. *J. Chem. Phys.* **1955**, *23*, 356–359.
(51) Leonov, A. I.; Siline, M. *Polymer* **2002**, *43*, 5521–5525.
(52) Mortensen, K. *J. Phys.: Condens. Matter* **1996**, *8*, A103–A124.
(53) Aharoni, S. M. *Macromolecules* **1983**, *16*, 1722–1728.
(54) Kimmich, R.; Fatkullin, N. *Adv. Polym. Sci.* **2004**, *170*, 1–113.
(55) Flory, P. F. *Principles of Polymer Chemistry*; Cornell University Press: Ithaca, NY, 1953.
(56) Brandrup, J.; Immergut, E. H.; Grulke, E. A.; Abe, A.; Bloch, D. R. *Polymer Handbook*, 4th ed.; John Wiley & Sons: New York, 2005.
(57) Prausnitz, J. M.; Lichtenthaler, R. N.; de Azevedo, E. G. *Molecular thermodynamics of fluid-phase equilibria*, 3rd ed.; Prentice-Hall PTR: Englewood Cliffs, NJ, 1999.
(58) Mokraoui, S.; Coquelet, C.; Valtz, A.; Hegel, P. E.; Richon, D. *Ind. Eng. Chem. Res.* **2007**, *46*, 9257–9262.
(59) Zhang, S.; Hiaki, T.; Kojima, K. *Fluid Phase Equilib.* **1998**, *149*, 27–40.
(60) Baulin, V. A.; Halperin, A. *Macromolecules* **2002**, *35*, 6432–6438.
(61) Berthod, A.; Tomer, S.; Dorsey, J. G. *Talanta* **2001**, *55*, 69–83.
(62) Corkill, J.; Goodmaann, J.; S.P.Harrod, D. *Trans. Faraday Soc.* **1963**, *60*, 202–207.
(63) Cheng, J.-S.; Chen, Y.-P. *Fluid Phase Equilib.* **2005**, *232*, 37.

(64) Chen, L.-J.; Lin, S.-Y.; Huang, C.-C.; Chen, E.-M. *Physicochem. Eng. Aspects* **1998**, *135*, 175–181.
(65) Chen, C. *AIChE J.* **1996**, *42*, 3231–3240.
(66) Li, X.-S.; Lu, J.-F.; Li, Y.-G.; Liu, J.-C. *Fluid Phase Equilib.* **1998**, *153*, 215–229.
(67) Gezae, A. Ph.D. Thesis; Universitat Rovira i Virgili, 2011